Making Indoor Maps with Portable Accelerometer and Magnetometer

Yiguang Xuan, Raja Sengupta, Yaser Fallah
Department of Civil and Environmental Engineering
University of California, Berkeley
Berkeley, California, 94720, U.S.A.
xuanyg@berkeley.edu, sengupta@ce.berkeley.edu, yaserpf@berkeley.edu

Abstract— **The paper describes algorithms required to enable the crowd sourcing of indoor building maps, i.e., where global positioning system (GPS) is not available. Nevertheless to enable crowd sourcing we use the 3-axis accelerometers and the 3-axis magnetometers available in many smart phones. Volunteers carry the phones while walking around in buildings, and use some application on their smart phones to send the data to a mapping server. We present the algorithms to obtain walking trajectories from the data by dead reckoning, and to estimate indoor maps with multiple walking trajectories.**

Keywords- crowd sourcing, indoor mapping, dead reckoning

I. INTRODUCTION

Open map systems (e.g., openstreetmap.org, waze.com) are viable today due to the rise of crowd sourcing. Open map systems combine two major sources of data: geographic information system (GIS) databases and motion trajectories contributed by the crowd. Any person with a global positioning system (GPS) receiver/logger on an increasing number of consumer devices can record his/her own trajectory and send it in to help an open map system. However, this approach does not work when the GPS signal is poor or not available, for example, within buildings. Thus the objective of this paper is to explore ways to crowd source indoor maps without relying on GPS.

The literature shows how to navigate and map indoor environments with relative and absolute positioning technologies other than GPS. For example, [1] describes the use of laser to scan buildings from outside through windows and map the interior of buildings. The quality of the map depends on obstructions due to the windows. The work in [2] uses radio frequency (RF) ranging to measure the distance from a sensor worn by a person to multiple base stations, and then triangulate to localize the person, in a manner similar to GPS. The accuracy of the positioning depends on the severity of the multi-path effect. These mapping methods require the installation of a base station infrastructure.

In the relative positioning literature, maps are built using inertial navigation systems (INS) and imaging sensors such as vision, lidar, sonar, or radar. A robot equipped with such sensors navigates through the environment to be mapped without any absolute position measurement [3, 4, 5, 6]. Reference [7] describes the use of a compass and an accelerometer to locate personnel within buildings. The work is similar to ours, but requires the compass to be fixed with known orientation.

We focus on indoor mapping using smart phones. This paper describes the algorithms developed to crowd source indoor maps. We envisage people carrying these phones, installing an application and communicating data to the mapping server. Our algorithms utilize the 3-axis accelerometers and 3-axis magnetometers that are available on many smart phones (e.g. iPhone or G-Phone). We do not need prior information about the orientation of the sensors as in [7].

The rest of the paper is organized as below. Section 2 introduces the sensors involved; section 3 presents the methodology to produce walking trajectories with the sensors; section 4 describes how floor map is estimated; section 5 discusses the result.

II. SENSORS

The 3-axis accelerometer and the 3-axis magnetometer used in this study are integrated in a G-Phone. The G-Phone coordinate is defined as in Fig. 1: +x direction extends along

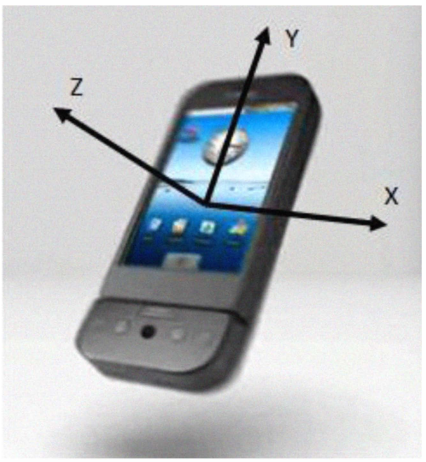

Figure 1. The G-Phone used in the experiment with its three axes.

978-1-4244-7879-8/10/$26.00 ©2010 IEEE

the short edge of the screen to the right; +y direction extends along the long edge of the screen to the front; +z direction extends perpendicularly out of the screen. The G-Phone measures its accelerations and magnetic intensity along the three axes at a frequency of about 46Hz. The bias in the magnetic intensity measurements is well documented [8, 9], and can be calibrated by simply rotating the G-Phone along its three axes.

During our study, volunteers walk around within the same building multiple times carrying the G-Phone. The logged data are used to map the building. We make the following assumptions to create an experiment simple enough for a proof of concept: (1) the map is restricted to one floor; (2) the hallways are straight, and are parallel or perpendicular to each other; (3) the orientation of the G-Phone is unknown, but is fixed or changes slowly with respect to the trunk of the volunteer (for example, as happens when carried in a chest pocket or backpack).

III. NAVIGATION

The methodology for navigation is described in three steps. First, the orientation of the G-Phone is estimated with the measurements of the gravity and the magnetic north. Second, the walking direction is estimated from the 3-axis acceleration with some human walking patterns. Finally, walking speed is estimated from its correlation with the acceleration. Then dead reckoning is applied to produce the walking trajectories.

A. Estimation of Phone Orientation

Besides the G-Phone coordinates, we define the world coordinate, with +E/+N/+U direction pointing to magnetic **e**ast/magnetic **n**orth/vertically **u**p. Thus the orientation of the G-Phone can be described by a transformation matrix

$$\mathbf{T} = \begin{bmatrix} e_X & e_Y & e_Z \\ n_X & n_Y & n_Z \\ u_X & u_Y & u_Z \end{bmatrix},$$

where unit vectors along the +E, +N, and +U direction can be expressed as $\mathbf{e} = [e_X \quad e_Y \quad e_Z]^T$, $\mathbf{n} = [n_X \quad n_Y \quad n_Z]^T$, and $\mathbf{u} = [u_X \quad u_Y \quad u_Z]^T$ respectively in the G-Phone coordinate. With this definition, $\mathbf{T}^T\mathbf{T} = \mathbf{I}$. Also, if a vector can be expressed as $\mathbf{V}_G = [V_X \quad V_Y \quad V_Z]^T$ in the G-Phone coordinate and as $\mathbf{V}_W = [V_E \quad V_N \quad V_U]^T$ in the world coordinate, then $\mathbf{V}_W = \mathbf{T}\mathbf{V}_G$ and $\mathbf{V}_G = \mathbf{T}^T\mathbf{V}_W$.

To estimate the orientation of the G-Phone, some prior knowledge is exploited: the gravity points into the –U direction; the magnetic north lie on the plane formed by the –U and +N directions. So we want to estimate **T**, with the measurements of gravity $\mathbf{G}_G = [G_X \quad G_Y \quad G_Z]^T$ and magnetic field $\mathbf{M}_G = [M_X \quad M_Y \quad M_Z]^T$, knowing that $\mathbf{G}_W = [0 \quad 0 \quad -G_U]^T$ and $M_W = [0 \quad M_N \quad -M_U]^T$. Interested reader can verify that the following procedure yield the estimate of **T**:

$$\mathbf{u} = \frac{-\mathbf{G}_G}{\|\mathbf{G}_G\|},$$

$$\mathbf{n} = \frac{\mathbf{M}_G - (\mathbf{u}^T\mathbf{M}_G)\mathbf{u}}{\|\mathbf{M}_G - (\mathbf{u}^T\mathbf{M}_G)\mathbf{u}\|},$$

$$\mathbf{e} = \mathbf{n} \times \mathbf{u},$$

$$\mathbf{T} = [\mathbf{e} \quad \mathbf{n} \quad \mathbf{u}]^T,$$

where × denotes cross product.

Note that the magnetic north is not the true north, and the magnetic declination angle (the difference between the magnetic north and the true north) is documented by location and by date [10].

B. Estimation of Walking Direction

Accelerometers have been widely used to predict human moving behavior [11, 12, 13]. Within this section, the accelerations along the 3 axes are used to predict the walking direction of the volunteer, with the knowledge of two human walking patterns. These walking patterns have been identified previously by researchers, but they have not been used to predict walking direction.

Define the volunteer coordinate: +AP (for anteroposterior) direction points to the front, +ML (for mediolateral) direction points to the left, and +V (for vertical) direction points up. We find that the acceleration along the ML axis always has the smallest root mean square (RMS) compared with the acceleration along the V or AP axis. For example, in one of our walking samples with speed 1.3 m/s, the RMS of the acceleration along the AP, ML, and V axes are 1.0 m/s^2, 0.6 m/s^2, and 2.4 m/s^2 respectively. Figure 4 of [14] confirms our finding, although the purpose of [14] is to estimate walking speed rather than to use this pattern to obtain the direction of walking. Since the average acceleration for motion with uniform speed is theoretically zero, the RMS can be interpreted as the intensity of motion. Thus the physical interpretation of this pattern is that there is less motion in the ML direction compared with AP and V directions.

Making use of this pattern, we carry out a principal component analysis (PCA) on (part of) the time series of the 3-D acceleration. PCA decomposes the 3-D acceleration into three principal components, so that the first principal component captures as much variance as possible, and the second principal component captures as much of the remaining variance as possible. Thus the third principal component is the estimate of the ML axis ($\overline{\mathrm{ML}}$). Among the first and second principal components, the one closer to gravity is the estimate of the V axis ($\overline{\mathrm{V}}$), and the other is the estimate of the AP axis ($\overline{\mathrm{AP}}$).

Now we have identified the axes $\overline{AP}$, $\overline{ML}$, and $\overline{V}$ of the volunteer coordinate. But these axes are bidirectional and we need to decide whether the walking direction is in the $+\overline{AP}$ direction or the $-\overline{AP}$ direction.

We further find out that during the walking process, the up and down movement along the V axis and the acceleration and deceleration along the AP axis are correlated. The acceleration along the AP axis is followed by the up movement along the V axis, then the deceleration along the AP axis, and then the down movement along the V axis. The process is shown with sample walking data in Fig. 2. Reference [15] confirmed this pattern with similar experiments, though the purpose of their study is to estimate the energy related to walking, not to predict walking direction.

Using this pattern, one can easily determine whether the walking direction is in the $+\overline{AP}$ direction or $-\overline{AP}$ direction, based on whether the gravity lies in the $+\overline{V}$ or $-\overline{V}$ direction. The estimated walking direction is then converted from the G-Phone coordinate into the world coordinate with the estimated transformation matrix **T** from Section 3.1.

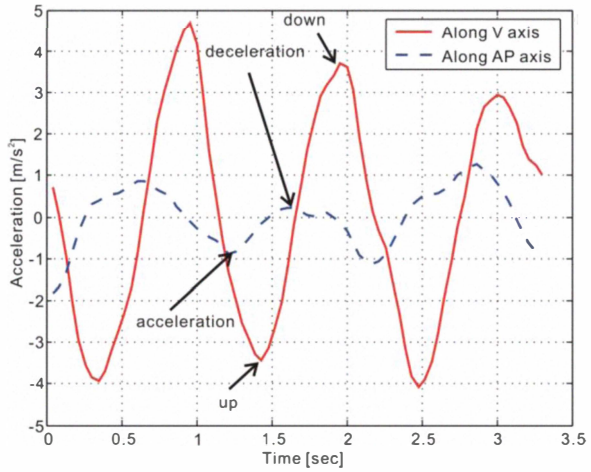

(a)

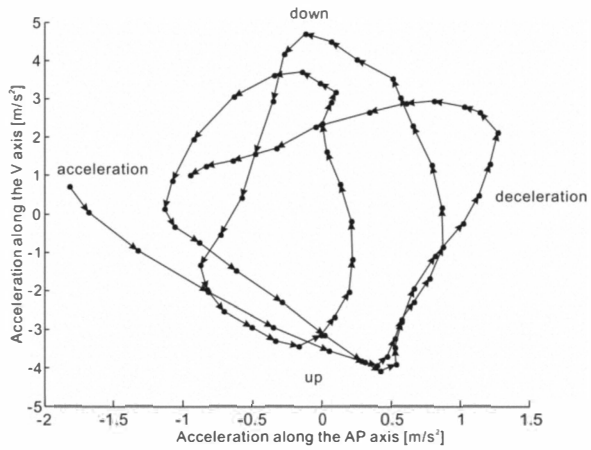

(b)

Figure 2. Walking pattern: correlated V-axis component and AP-axis component of acceleration. (a) V-axis and AP-axis components vs. time; (b) V-axis component vs. AP-axis component.

C. *Estimation of Walking Speed*

The walking speed is estimated with the RMS of the acceleration. The rationale is that the RMS of the acceleration, which is an indicator of motion intensity, is correlated with walking speed. We have several volunteers walking at different speeds with the G-Phone in hand. One volunteer is asked to walk on a treadmill with preset speeds. Other volunteers are asked to walk along hallways with relatively uniform speed. Their speed is calculated by timing their walking over a predetermined distance. Fig. 3 shows these data.

We then fit the data assuming the relationship between the RMS of the acceleration and the speed is linear. The linear relation is adopted only for simplicity. Complicated regression analysis should improve the estimation. The result of the fitting is also shown in Fig. 3, and is used later for speed estimation. This method to estimate speed with the RMS of the acceleration is not new either; see [14, 16, 17] for similar studies.

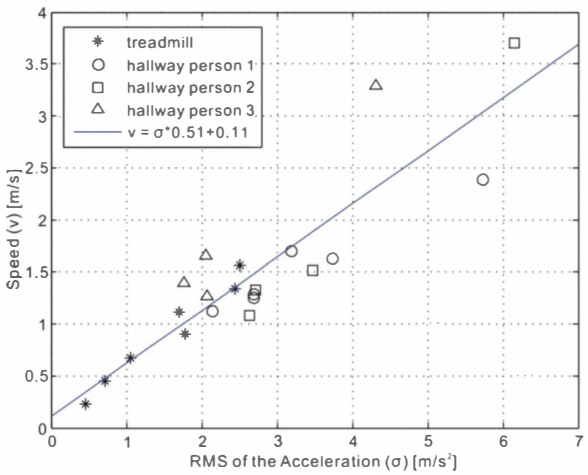

Figure 3. Speed calibration with the RMS of the acceleration.

D. *Post-processing*

After obtaining the walking direction and walking speed respectively, dead reckoning is applied to obtain the walking trajectories during the post-processing. Necessary corrections are made to the trajectories with the assumption that the hallways are straight and any that two hallways are parallel or perpendicular.

The walking direction is represented by the azimuth angles, with 0, $\pi/2$, π, and $3\pi/2$ indicating true north, east, south, and west. Fig. 4a shows the azimuth angle versus time for a sample walking trajectory. First, we discretize the azimuth angle by clustering, with the assumption that hallways are straight. The center of the clusters are shown in Fig. 4a, while the discretized azimuth angle versus time is shown in Fig. 4b.

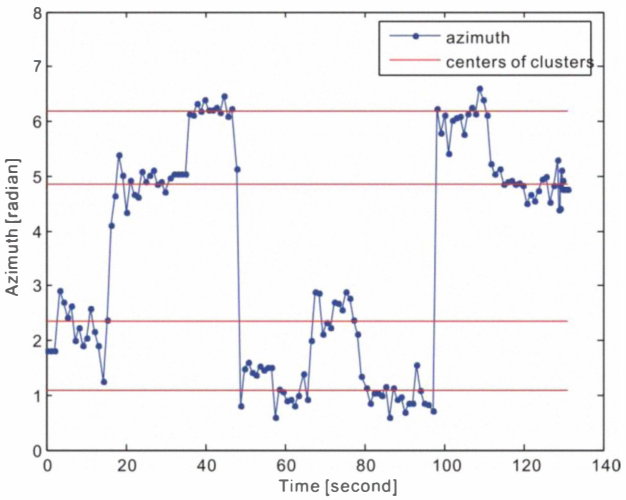

(a)

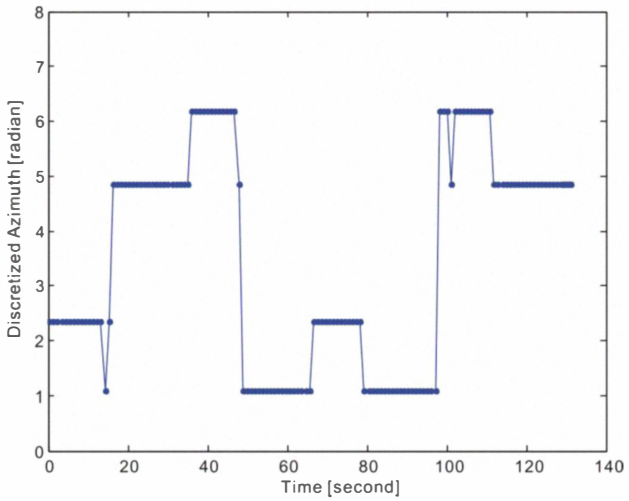

(b)

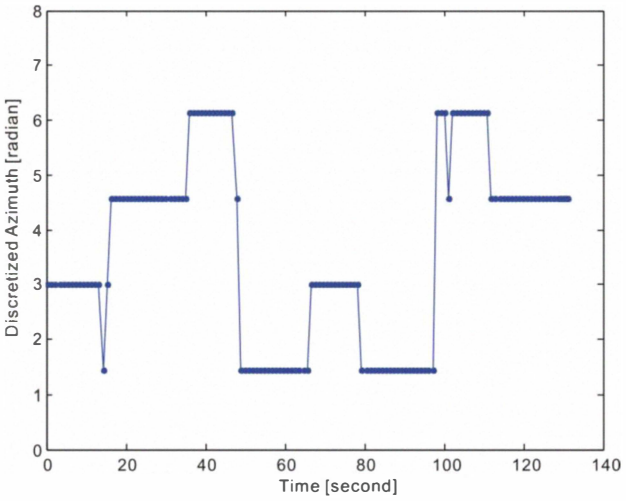

(c)

Figure 4. Adjustment of azimuth angle. (a) clustering of azimuth angle; (b) discretized azimuth angle; (c) discretized azimuth angle after correcting for distortion of the local magnetic field.

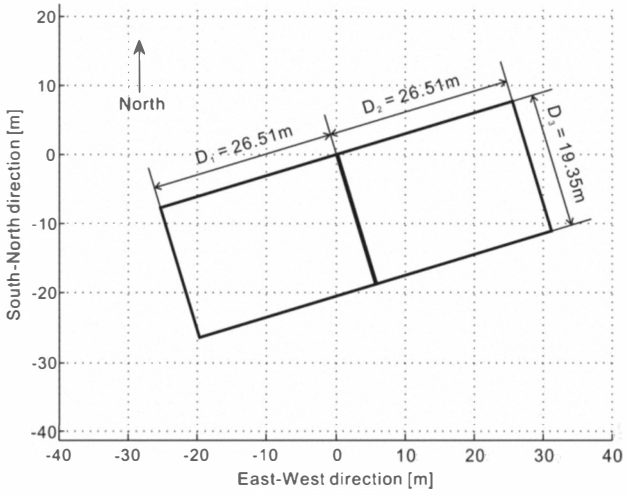

(a)

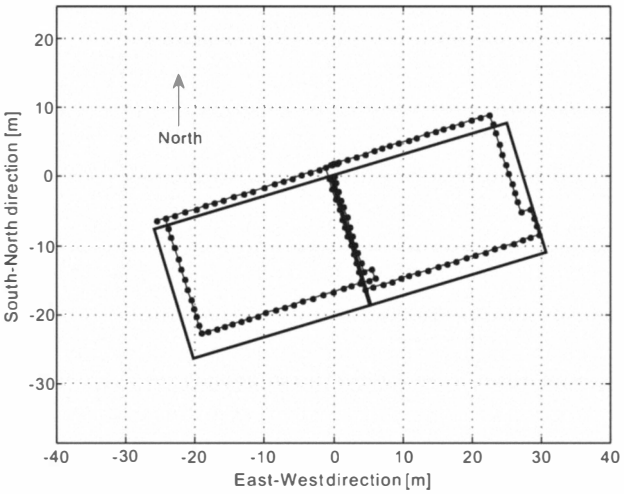

(b)

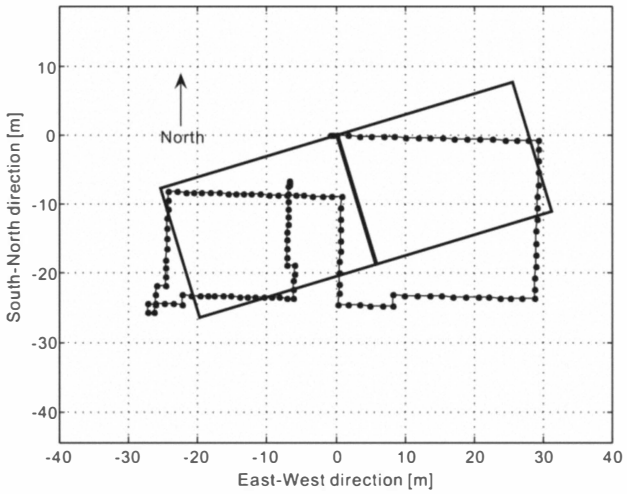

(c)

Figure 5. True floor map and walking trajectories from the 5th floor of Davis Hall, UC Berkeley. (a) true floor map; (b) one sample walking trajectory; (c) another sample walking trajectory.

Note that the discretized azimuth angles can be neither parallel nor perpendicular due to distortion of the local magnetic field. To account for this problem, we define an independent orientation parameter to be the orientation of an arbitrary hallway. Then the orientation of all the hallways can be expressed by this orientation parameter plus or minus integer times of $\pi/2$. Thus we use the measured azimuth angles to estimate this parameter, and then express the orientation of all the hallways with the estimate of this orientation parameter. This adjustment is shown in Fig. 4c.

A volunteer walked the hallways of the 5th floor of Davis Hall at the University of California, Berkeley, holding the G-Phone in hand. During the walking process, the phone is held still with respect to the trunk of the volunteer, but the orientation of phone is not used in the study. The true floor map consists of two side-by-side rectangles, as shown in Fig. 5a. The aforementioned method is used to obtain walking trajectories, two of which are shown in Fig. 5b and Fig. 5c. Note that the north shown in the figures is the true north, after correcting for the magnetic declination angle.

IV. Estimation of Floor Map

One way to model a floor map is to represent each leg of the hallways with a length parameter and an orientation parameter. Not all parameters are independent though. Since the hallways form loops, not all length parameters are independent. For example, only three length parameters are needed to determine the floor map shown in Fig. 5a. Also, only one independent orientation parameter is needed. We will use the orientation of the northbound hallway during our study.

Here we propose a method to estimate the dimension of floor maps with multiple walking trajectories, to account for the inaccuracies in the estimation of the individual walking trajectories. We assume the walking always starts and ends at the same location, e.g., the elevators or the entrance of buildings. To integrate the floor map into a geo-coded outside map, this location needs to be known in some global reference, e.g., from GPS or Wi-Fi hotspots.

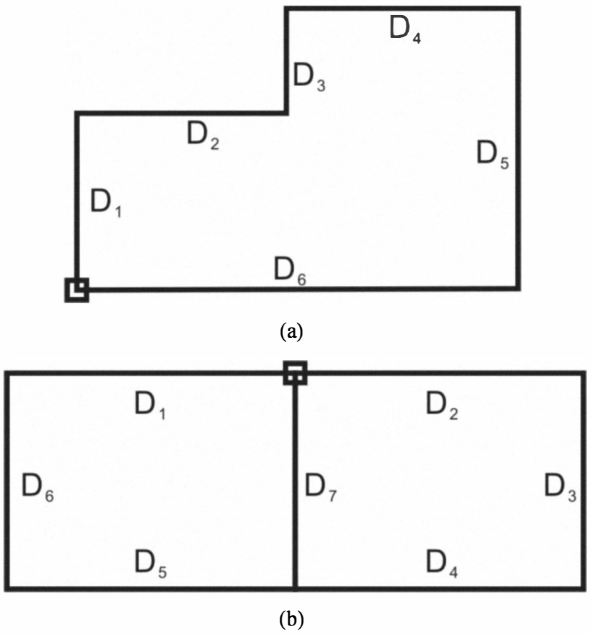

Figure 6. Imaginary floor map. (a) with only one loop; (b) with two loops (the floor map for the 5th floor of Davis Hall).

The floor map is divided into loops (Fig. 6a shows one such loop). Each leg of a loop is represented with unknown length parameters D_i (i = 1 to n) and known azimuth angles a_i (i = 1 to n). Let us assume that leg i is walked m_i times and the j^{th} measurements of D_i is L_{ij} (j = 1 to m_i). Then the estimation of D_i's can be formulated as a constrained optimization problem so that the total sum of squared errors is minimized:

$$\{D_i^*\} = \arg\min \sum_{i=1}^{n}\sum_{j=1}^{m_i}(D_i - L_{ij})^2$$
$$\text{s.t.} \quad \sum_{i=1}^{n} D_i \cos(a_i) = 0, \quad \sum_{i=1}^{n} D_i \sin(a_i) = 0.$$

The singularity problem may arise with quadratic optimization when the number of parameters is huge. But it is unlikely to happen because in our application the number of parameters is generally much less than the number of measurements.

For our example of the 5th floor of Davis Hall, as shown in Fig. 6b, it turns out that the sample mean is the best estimate for D_i, due to its simple geometry:

$$\{D_i^*\} = \arg\min \sum_{i=1}^{n}\sum_{j=1}^{m_i}(D_i - L_{ij})^2$$
$$\text{s.t.} \quad D_1 = D_5, \quad D_2 = D_4, \quad D_3 = D_6 = D_7.$$

$$\Rightarrow \begin{cases} D_1^* = \dfrac{1}{m_1 + m_5}\left(\sum_{j=1}^{m_1} L_{1j} + \sum_{j=1}^{m_5} L_{5j}\right) \\ D_2^* = \dfrac{1}{m_2 + m_4}\left(\sum_{j=1}^{m_2} L_{2j} + \sum_{j=1}^{m_4} L_{4j}\right) \\ D_3^* = \dfrac{1}{m_3 + m_6 + m_7}\left(\sum_{j=1}^{m_3} L_{3j} + \sum_{j=1}^{m_6} L_{6j} + \sum_{j=1}^{m_7} L_{7j}\right) \end{cases}$$

Fig. 7a – Fig. 7c show how the estimates of D_1, D_2, and D_3 converge to their true values with increasing walking samples. The vertical axes show the estimate of the hallway lengths with the given number of walking samples collectively. We see that with just six walking samples, the length parameters can be estimated with a relative standard error of 4%.

Similarly, the orientation parameter is estimated with the measured azimuth angles as described in the previous section. The estimate of the orientation of the northbound hallway is shown in **Error! Reference source not found.**d. With six walking samples, the orientation parameter can be estimated with a standard error of 0.074 radian (about 4 degrees).

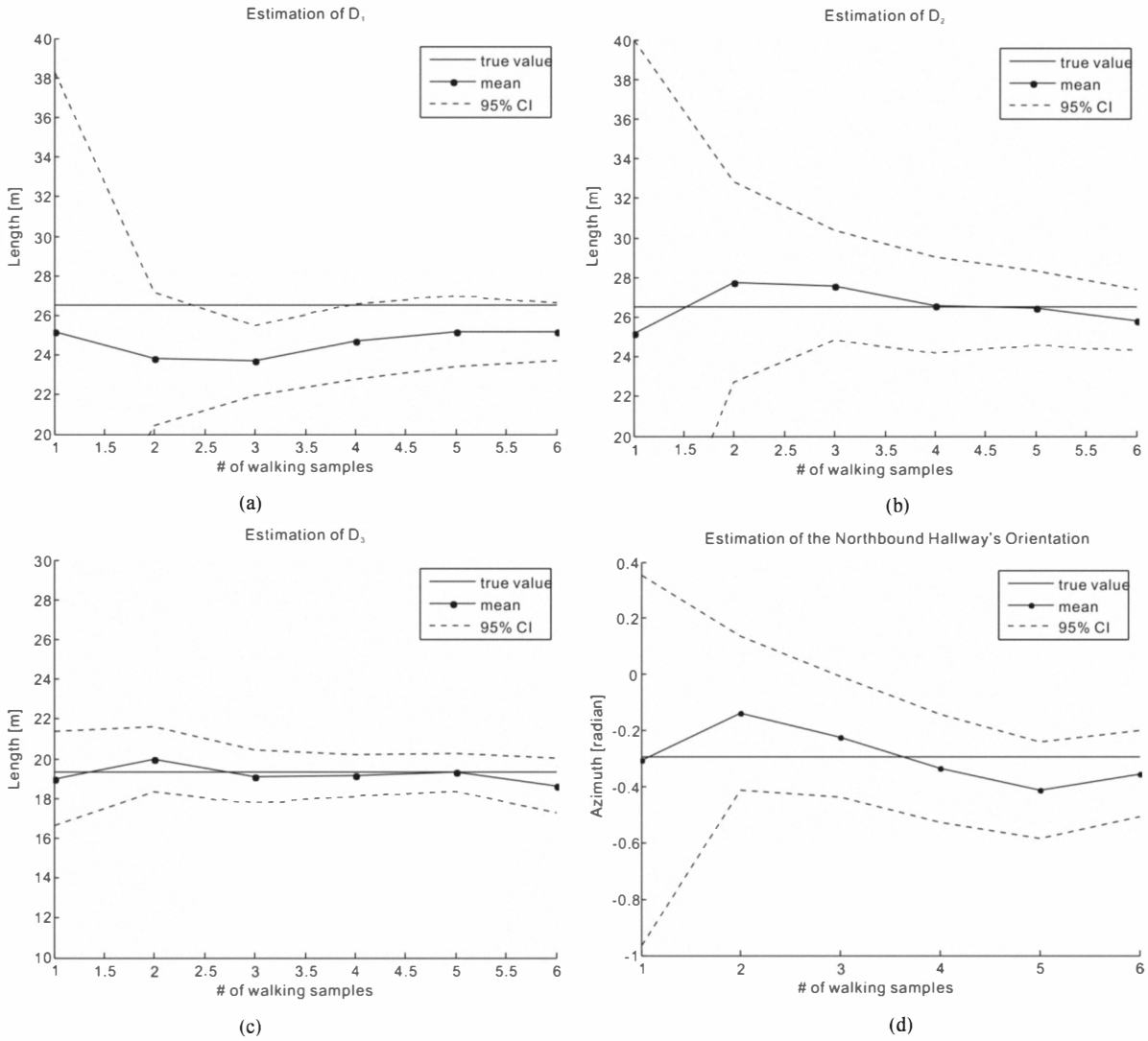

Figure 7. Estimation of the length and orientation parameters vs. the number of walking samples used for estimation. (a) estimation of D_1; (b) estimation of D_2; (c) estimation of D_3; (d) estimation of the orientation of the northbound hallway.

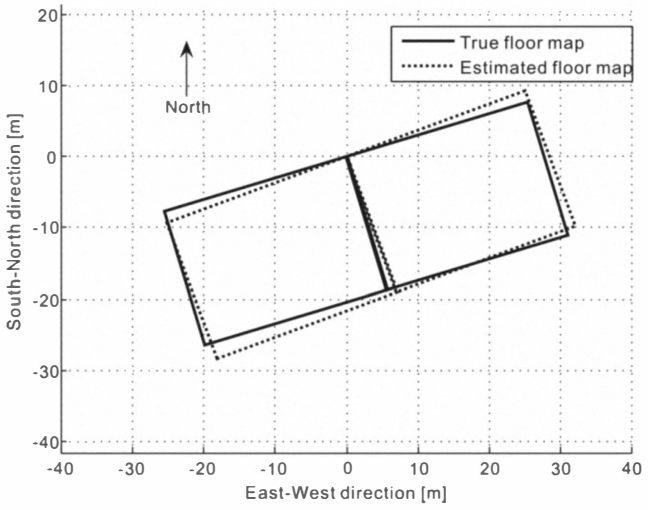

Figure 8. Estimated vs. true floor map of the 5th floor of Davis Hall, UC Berkeley.

With just six walking samples, the estimated floor map has $\overline{D_1}$ = 25.16m, $\overline{D_2}$ = 25.84m, $\overline{D_3}$ = 18.65m. The estimated orientation of the northbound hallway is -0.3538 radian (about -20.3 degrees). The estimates are comparable with the true floor map with D_1 = 26.51m, D_2 = 26.51m, D_3 = 19.35m, and the orientation of the northbound hallway -0.2934 radian (about -16.8 degrees). The estimated and true floor maps are shown together in **Error! Reference source not found.**.

V. DISCUSSION

A successful project to crowd source indoor maps includes at least the following problems: the relative mapping, the global mapping, and the incentive problem. The relative mapping problem is to make a map with the correct proportions and orientation. This problem is the focus of the paper. The global mapping problem locates the relatively correct map in a common coordinate system such as the GPS Universal Transverse Mercator (UTM) system. We intend to

address this problem next by using GPS readings at the entrances and exits of buildings (trajectory starting and ending point) and Wi-Fi hotspot readings. The incentive problem is about how to motivate the crowd to collect walking data and send them to a mapping server. Waze.com does an excellent job on this problem.

The contribution of this paper is a solution to the relative mapping problem. We proposed a methodology to estimate the lengths and orientations of the hallways. We then validate it by showing that we are able to estimate a floor map accurately with just a few walking samples. We compute the map for one floor requiring the correct estimation of three lengths and one orientation. The length parameters are estimated with a relative standard error of 4%, and the orientation parameter is estimated with a standard error of 0.074 radian (about 4 degrees), with six walking samples. The methodology should be generally applicable to other floors as long as the lengths and orientations of hallways can be estimated correctly. We expect the difference from floor to floor to lie in the number of samples required to obtain a correct map.

REFERENCES

[1] M. Johnston and A. Zakhor, "Estimating building floor-plans from exterior using laser scanners," SPIE Electronic Imaging Conference, 3D Image Capture and Applications, 2008.

[2] J. Duckworth, D. Cyganski, S. Makarov, W. Michalson, J. Orr, et al., " WPI Precision Personnel Locator System – Evaluation by First Responders," The 20th International Technical Meeting of the Institute of Navigation Satellite Division, 2007.

[3] S. Thrun, W. Burgard and D. Fox, "A real-time algorithm for mobile robot mapping with applications to multi-robot and 3D mapping," IEEE International Conference on Robotics and Automation, vol. 1, pp. 321-328, 2000.

[4] N. Naikal, J. Kua, G. Chen and A. Zakhor, "Image Augmented Laser Scan Matching for Indoor Dead Reckoning," International Conference on Intelligent Robots and Systems, 2009.

[5] S. Li, T. Kanbara and A. Hayashi, "Making a local map of indoor environments by swiveling a camera and a sonar," IEEE International Conference on Intelligent Robots and Systems, vol. 2, pp. 954-959, 1999.

[6] Stanford Research Institute, Centibots, http://www.ai.sri.com/centibots/index.html, 2004.

[7] I. Sharp, "Tracking method and apparatus," US patent application no. 10/547,238, 2004.

[8] J. D. Graves, "Design and control of a vehicle for neutral buoyancy simulation of space operations," M.S. thesis, University of Maryland at College Park, 1997.

[9] J. H. Wang and Y. Gao, "GPS-based land vehicle navigation system assisted by a low-cost gyro-free INS using neural network," Journal of Navigation, vol. 57, pp. 417-428, 2004.

[10] National Geographic Data Center, NOAA Satellite and Information Service, http://www.ngdc.noaa.gov/geomagmodels/struts/calcDeclination.

[11] J. R. W. Morris, "Accelerometry - A technique for the measurement of human body movements," Journal of Biomechanics, vol. 6, pp. 729-736, 1973.

[12] A. Godfrey, R. Conway, D. Meagher and G. Olaighin, "Direct measurement of human movement by accelerometry," Medical Engineering & Physics, vol. 30, pp. 1364-1386, 2008.

[13] J. J. Kavanagh and H. B. Menz, "Accelerometry: A technique for quantifying movement patterns during walking," Gait & Posture, vol. 28, pp. 1-15, 2008.

[14] R. Moe-Nilssen, "A new method for evaluating motor control in gait under real-life environmental conditions Part 2: Gait analysis," Clinical Biomechanics, vol. 13, no. 4-5, pp. 328-335, 1998.

[15] G. Cavagna, F. Saibene and R. Margaria, "External work in walking," Journal of Applied Physiology, vol. 18, pp. 1-9, 1963.

[16] Y. Schutz, S. Weinsier, P. Terrier and D. Durrer, "A new accelerometric method to assess the daily walking practice," International Journal of Obesity, vol. 26, pp. 111-118, 2002.

H. B. Menz, S. R. Lord and R. C. Fitzpatrick, "Acceleration patterns of the head and pelvis when walking on level and irregular surfaces," Gait Posture, vol. 18, no. 1, pp. 35-46, 2003.